



# Research on Automotive Bearing Fault Diagnosis Based on the Improved SSA-VMD Algorithm

Weidong Huang<sup>1</sup>, Yiqun Cai<sup>2,\*</sup>

<sup>1</sup> Upower Energy Technology (Guang Zhou) Co.,Ltd., Guangzhou, 510000, CHINA

<sup>2</sup> Corresponding, University of Florida, Herbert Wertheim College, FL, 32608, USA,

Email: yiqun.cai@ufl.edu

**Abstract:** Due to the complexity and variability of automotive bearing fault vibration signals, as well as the challenges in feature extraction, a novel automotive bearing fault diagnosis method based on an improved SSA-VMD algorithm is proposed in this paper. Firstly, the number of modes (K) and the penalty factor ( $\alpha$ ) in the variational mode decomposition (VMD) algorithm are optimized by the Sparrow Search Algorithm (SSA). Secondly, the VMD using optimized parameters is used to decompose the automotive bearing fault vibration signal into a series of modal components. Modal components with larger kurtosis values are selected for reconstruction and feature extraction. Lastly, the feature vectors are input into a kernel extreme learning machine (KELM) model for fault recognition. A comparative analysis is conducted between the improved SSA-VMD method and the original SSA-VMD method in automotive bearing fault diagnosis. Experimental results demonstrate that the improved SSA-VMD method is satisfactory in extracting characteristic information from automotive bearing fault vibration signals and achieves higher fault diagnosis accuracy.

**Keywords:** *Automotive Bearing; Improved SSA-VMD Algorithm; Refined Composite Multi-Scale Sample Entropy; Fault Diagnosis.*

## 1. Introduction

With the rapid development of the modern automotive industry, the safety and reliability of automobiles have attracted increasingly concerns. As a key component in the automotive drivetrain system [1], automotive bearings significantly influence the safety and performance of the vehicle. However, due to the long-term operation of automotive bearings under high speed, heavy load, and complex working conditions, their failure rate is relatively high [2]. Therefore, timely and accurate diagnosis of automotive bearing faults is crucial. To effectively extract fault characteristic information from automotive bearings and improve fault diagnosis accuracy, this paper focuses on the decomposition of automotive bearing vibration signals and fault diagnosis. Automotive bearing fault vibration signals are often accompanied by significant noise, necessitating signal decomposition and denoising treatment. In 2014, a novel signal decomposition method, Variational Mode Decomposition (VMD), was proposed by Dragomiretskiy et al. to address the signal denoising problem [3]. The VMD algorithm

effectively resolves two major issues in Empirical Mode Decomposition (EMD) and Local Mean Decomposition (LMD), namely endpoint effects and mode overlapping. As a result, VMD has been widely applied in various signal decomposition tasks. However, the number of modes (K) and the penalty parameter ( $\alpha$ ) in the VMD algorithm significantly impact the decomposition results, and both parameters are uncertain. Therefore, optimizing the combination of these parameters is of great importance. General methods for determining the optimal combination of K and  $\alpha$  typically involve heuristic algorithms. For example, Li Hong et al. [4] used the Grey Wolf Optimizer (GWO) to search for the optimal decomposition parameters for VMD, which significantly improved decomposition performance using a central frequency observation method. However, this algorithm is prone to local optima and suffers from low computational efficiency. In 2023, G Huazhan [5] proposed the Sparrow Search Algorithm (SSA) to optimize the VMD parameters K and  $\alpha$ , and combined it with Extreme Learning Machine (ELM) for bearing fault diagnosis on data from Case Western Reserve University. This method offers high solution accuracy and novelty, but still faces issues such as falling into local optima. To address the problem of heuristic algorithms being prone to local optima in optimizing VMD, this paper proposes an improved SSA-VMD algorithm for parameter optimization.

Since the original SSA-VMD algorithm suffers from a reduction in population diversity during the later stages of iteration [6], which reduces the global search ability and affects computational efficiency, potentially leading to local optima, this paper introduces a t-distribution mutation strategy into the target position update process. The t-distribution operator enhances the disturbance ability, generating new mutated individuals to update the target positions. This improvement enhances both the global and local search performance of the algorithm, thereby increasing the solution accuracy and obtaining the optimal parameter combination [K,  $\alpha$ ] for VMD.

Specifically, the optimized VMD method is used to decompose the automotive bearing fault vibration signals into multiple modal components. The kurtosis values of each component are calculated, and those with higher kurtosis are selected for signal reconstruction. The reconstructed signal is then analyzed using the refined composite multi-scale sample entropy (RCMSE) method to extract feature vectors [7]. These feature vectors are subsequently input into a Kernel Extreme Learning Machine (KELM) for fault classification[8]. Finally, a comparison is made between the improved SSA-VMD method and the original SSA-VMD method to assess the performance of the proposed approach.

## 2. Theoretical background

### 2.1 Variational Mode Decomposition

The VMD algorithm decomposes time series within a fixed variational framework and generates several intrinsic mode functions (IMFs) as signal components. Each component is an amplitude-frequency modulation function, which satisfies the definition of an intrinsic mode function (IMF) [9].

The model expression of the Variational Mode Decomposition (VMD) algorithm is as follows: Where  $u_k$  represents the modal components obtained after decomposition;  $\omega_k$  represents the central frequency of each IMF component.

$$\begin{cases} \min_{\{u_k\}, \{\omega_k\}} \left\{ \sum_k \left\| \partial_t \left[ \left( \delta(t) + \frac{j}{\pi t} \right) u_k(t) \right] e^{-j\omega_k t} \right\|_2^2 \right\} \\ \text{s.t.} \sum_k u_k(t) = f \end{cases} \quad (1)$$

To solve the VMD model, the Lagrangian function is introduced to simplify the constrained problem and convert it into an unconstrained problem. The Lagrangian function is shown in equation (2):

$$L(\{u_k\}, \{\omega_k\}, \lambda) = \alpha \sum_k \left\| \partial_t \left[ \left( \delta(t) + \frac{j}{\pi t} \right) u_k(t) \right] e^{-j\omega_k t} \right\|_2^2 + \left\| f(t) - \sum_k u_k(t) \right\|_2^2 + \langle \lambda(t), f(t) - \sum_k u_k(t) \rangle \quad (2)$$

Where  $\alpha$  is a quadratic penalty parameter that ensures signal reconstruction accuracy even in the presence of Gaussian noise;  $\lambda(t)$  is the multiplier operator.

The alternating operator method is used to solve for the extrema of equation (2). By iteratively updating  $u_k^{n+1}$ ,  $\omega_k^{n+1}$ , and  $\lambda^{n+1}$ , the extremum points of the function are obtained. The update for  $u_k^{n+1}$  is given by equation (3):

$$u_k^{n+1} = \arg \min_{u_k \in X} \left\{ \alpha \left\| \partial_t \left[ \left( \delta(t) + \frac{j}{\pi t} \right) u_k(t) \right] e^{-j\omega_k t} \right\|_2^2 + \left\| f(t) - \sum_i u_i(t) + \frac{\lambda(t)}{2} \right\|_2^2 \right\} \quad (3)$$

Fourier transform is applied to equation (3) to calculate the optimal solution for the quadratic optimization problem, as shown in equation (4):

$$\hat{u}_k^{n+1}(\omega) = \frac{\hat{f}(\omega) - \sum_{i \neq k} \hat{u}_i(\omega) + \frac{\hat{\lambda}(\omega)}{2}}{1 + 2\alpha(\omega - \omega_k)^2} \quad (4)$$

The center frequency of each IMF component is computed as follows:

$$\omega_k^{n+1} = \frac{\int_0^\infty \omega |\hat{u}_k(\omega)|^2 d\omega}{\int_0^\infty |\hat{u}_k(\omega)|^2 d\omega} \quad (5)$$

Where  $\omega_k^{n+1}$  represents the central frequency spectrum of each component. The Fourier inverse transform is applied to  $\{\hat{u}_k(\omega)\}$  to solve for the corresponding time-domain signal components  $\{u_k(t)\}$ .

The steps of the VMD algorithm are as follows:

**Step 1:** Initialize  $\{\hat{u}_k^1\}, \{\omega_k^1\}, \{\hat{\lambda}^1\}$  and  $n$ ;

**Step 2:** Iteratively update  $u_k$  and  $\omega_k$  using equations (1) and (2)

**Step 3:** Update  $\lambda$  using equation (6)

$$\hat{\lambda}^n(\omega) + \tau [\hat{f}(\omega) - \sum_k \hat{u}_k^{n+1}(\omega)] \rightarrow \hat{\lambda}^{n+1}(\omega) \quad (6)$$

Where  $\tau$  represents the noise tolerance level.

**Step 4:** Define the convergence criterion  $\varepsilon > 0$  if

$$\sum_k \frac{\|\hat{u}_k^{n+1} - \hat{u}_k^n\|_2^2}{\|\hat{u}_k^n\|_2^2} < \varepsilon \quad (7)$$

Then the iteration stops. Otherwise, return to step 2 and continue iterating.

## 2.2 Improved SSA Optimization for VMD

As mentioned in the introduction, the mode  $K$  and the penalty factor  $\alpha$  are key factors affecting the decomposition performance of the VMD algorithm. Since the choice of these two parameters is uncertain, determine optimal values for them is crucial. To address the issue of traditional heuristic algorithms for optimizing VMD often falling into local optima, this paper proposes using an improved SSA-VMD algorithm to optimize the parameters  $[K, \alpha]$  of VMD.

### (1) Issues with the original SSA-VMD algorithm

The original SSA-VMD algorithm suffers from reduced population diversity in the later stages of iterations, leading to higher individual repetition rates. This reduces the global search capability of the algorithm, affecting its computational efficiency and causing it to fall into local optima. To overcome this issue, this paper introduces a t-distribution mutation strategy into the target position update mechanism [10]. The t-distribution operator helps generate mutated new individuals, which are used to update the target positions. This enhances the global and local search capabilities of the SSA-VMD algorithm and improves its solution accuracy, leading to the optimal combination of VMD parameters  $[K, \alpha]$ .

### (2) Details of the algorithm improvements

To address the problem of reduced population size in the later stages of the algorithm, a t-distribution mutation strategy is introduced into the target position update process to generate new individuals. These new individuals help maintain population diversity, enhancing the algorithm's global search ability. By using the current population to mutate the original individuals, the algorithm avoids getting trapped in local optima and improves its overall optimization ability.

The improved SSA-VMD algorithm uses the iteration count as a degree of freedom parameter. In the early stages of the algorithm, the smaller value of  $t$  acts similarly to a Cauchy mutation operator, enabling the generation of new individuals with strong local search capabilities. In the later stages, the larger value of  $t$  acts like a Gaussian mutation operator, allowing the generation of new individuals with strong global search capabilities. This ensures the algorithm has both global search ability and improved local search performance, which helps to update the target position and improve the overall solution accuracy.

Therefore, in this paper, the improved SSA-VMD algorithm is used to optimize parameters, with the minimal value of the ratio of envelope entropy to kurtosis as the fitness function for optimizing the VMD parameters  $[K, \alpha]$ . The algorithm steps are as follows:

**Step 1:** Initialize the algorithm's population, iteration count, ratio of predators to joiners, and the sparrow group position vector  $[K_0, \alpha_0]$ .

**Step 2:** Calculate the current fitness value of the algorithm (the minimal value of the VMD envelope entropy to kurtosis ratio) and sort the fitness values in ascending order.

**Step 3:** Select the sparrow with the maximum fitness value as the discoverer. Use equation (8) to update its position:

$$X_{i,j}^{t+1} = \begin{cases} X_{i,j} \cdot \exp\left(-\frac{i}{\alpha \cdot \text{iter}_{\max}}\right), & \text{if } R_2 < st \\ X_{i,j} + Q \times L, & \text{if } R_2 > st \end{cases} \quad (8)$$

Where  $t$  represents the current iteration number;  $j = 1, 2, 3, \dots, d$ ;  $\text{iter}_{\max}$  is the maximum number of iterations;  $X_{i,j}$  is the position of sparrow  $i$  in dimension  $j$ ;  $R_2$  and  $s_t$  represent the alert and safety threshold values, respectively.

**Step 4:** Select the remaining sparrows as joiners. Update their positions using equation (9):

$$X_{i,j}^{t+1} = \begin{cases} Q \cdot \exp\left(\frac{X_{\text{worst}} - X_{i,j}^t}{\alpha \cdot \text{iter}_{\max}}\right), & \text{if } i > n/2 \\ X_P^{t+1} + |X_{i,j} - X_P^{t+1}| \cdot A^+ \cdot L, & \text{otherwise} \end{cases} \quad (9)$$

where:  $X_P$  is the optimal position corresponding to the discoverer sparrow;  $X_{\text{worst}}$  is the worst position corresponding to the discoverer sparrow.

**Step 5:** The scout sparrow is randomly selected. Its position is updated using equation (10):

$$X_{i,j}^{t+1} = \begin{cases} X_{\text{best}}^t + \beta \cdot |X_{i,j}^t - X_{\text{best}}^t|, & \text{if } f_i > f_g \\ X_{i,j}^t + K \cdot \left( \frac{|X_{i,j}^t - X_{\text{worst}}^t|}{(f_i - f_w) + \varepsilon} \right), & \text{if } f_i = f_g \end{cases} \quad (10)$$

Where  $X_{\text{best}}$  is the best position corresponding to the scout sparrow;  $\beta$  is the step size control parameter for the algorithm.

**Step 6:** Check if the condition  $\text{rand} < p$  is satisfied. If it is, apply the adaptive t-distribution mutation strategy to generate mutated individuals and replace the original individuals. If not, retain the original individuals.

**Step 7:** Calculate the current fitness value (the minimal value of the VMD envelope entropy to kurtosis ratio) and update the sparrow positions.

**Step 8:** Check if the algorithm has reached the optimal condition. If satisfied, terminate and output the optimal VMD parameter combination  $[K, \alpha]$ . Otherwise, return to Step 2 and repeat Steps 2-7.

The flowchart of the procedure is shown in Figure 1.

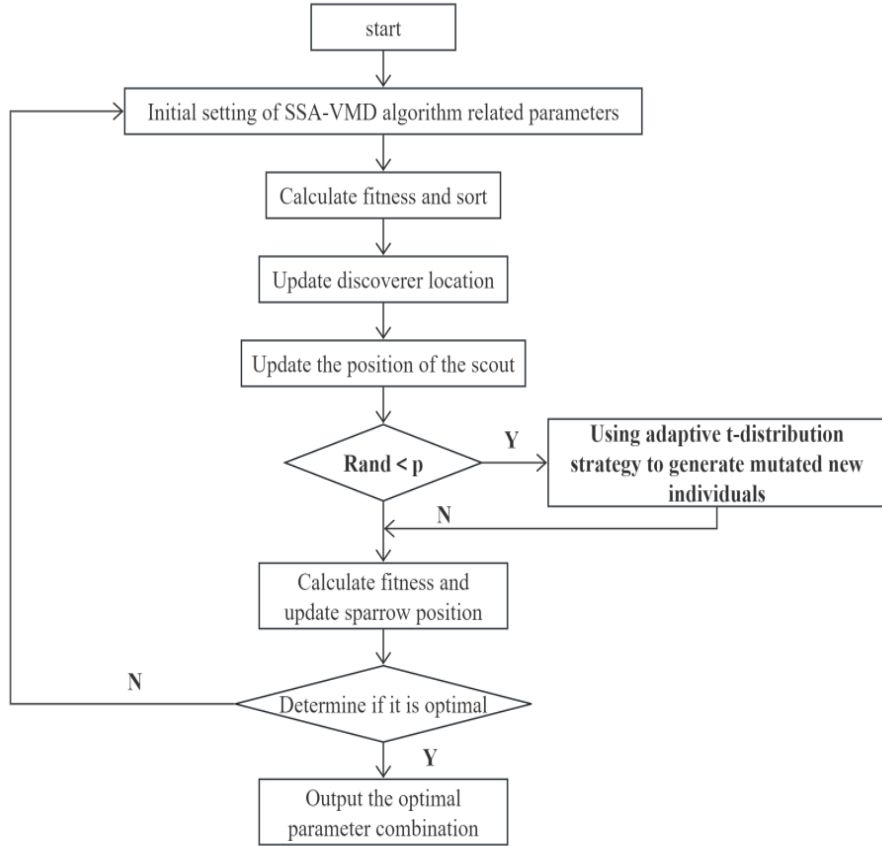


Fig 1 Flow chart of the improved SSA-VMD algorithm

### 3. Experimental verification of the proposed method

#### 3.1 Data Source for Fault Diagnosis

This study focuses on automotive bearing faults, with experimental data sourced from vibration signals of automotive bearings collected in the authors' laboratory. The data was obtained through fault simulation experiments conducted on the bearings of a famous automobile, provided by the laboratory's research team [11-12]. The bearing fault simulation was performed using worn-out bearings from the No. 1 unit, and faults were simulated under various bearing clearance conditions. These faults included large clearance in the first and second-stage connecting rod big-end bearings, as well as large clearance in the first and second-stage connecting rod small-end bearings. A total of four different bearing clearance fault conditions were simulated. In addition to these fault conditions, vibration data for a normally functioning bearing was also collected for comparison. The vibration signals corresponding to the following operating conditions were obtained: 1. Normal condition (Normal); 2. First class connecting rod big-end bearing clearance is large (FCB); 3. Second class connecting rod big-end bearing clearance is large (SCB); 4. First class connecting rod small-end bearing clearance is large (FCS); 5. Second class connecting rod small-end bearing clearance is large (SCS). The example time-domain vibration signals for each operating condition are shown in Figure 3.



Fig 2. Experiment condition of the study

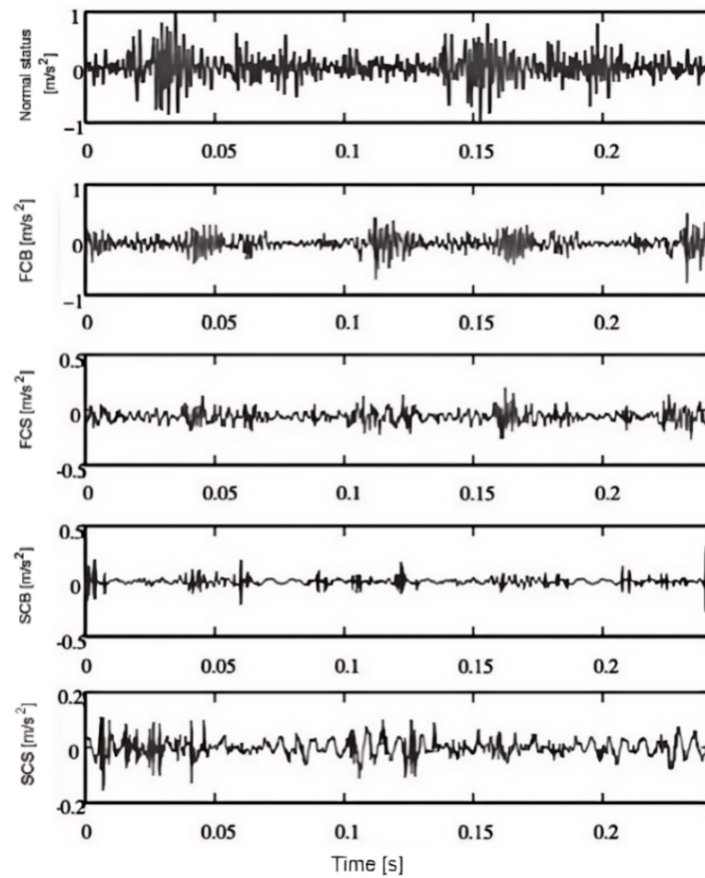


Fig 3 Time domain diagram corresponding to five working conditions

### 3.2 Optimal parameters

The optimal parameter combination  $[K_0, \alpha_0]$  for the five different bearing vibration states of the automotive bearings is determined using the improved SSA-VMD algorithm. In this study, the number of iterations is set to 80. Due to the inherent randomness of the algorithm's optimization process [13], the best parameter combination  $[K_0, \alpha_0]$  is obtained by averaging the results over 20

runs. The number of modes  $K$  is set in the range of [3,10], with integer values, and the penalty factor  $\alpha$  is set in the range of [500,6500]. The resulting optimal parameters are shown in Table 1.

Table 1 Optimal parameter combination  $[K_0, \alpha_0]$

Type of data	$[K_0, \alpha_0]$
Normal	[6,3691]
FCB	[7,4537]
SCB	[6,5200]
FCS	[6,6372]
SCS	[3,2690]

### 3.3 Feature extraction from Vibration Signals

In this section, the analysis results of a first-stage connecting rod big-end bearing clearance condition is set as a visual example. The vibration signals of the corresponding status are processed using both the original SSA-VMD and improved SSA-VMD algorithms, and the results are shown in Figures 4 and 5.

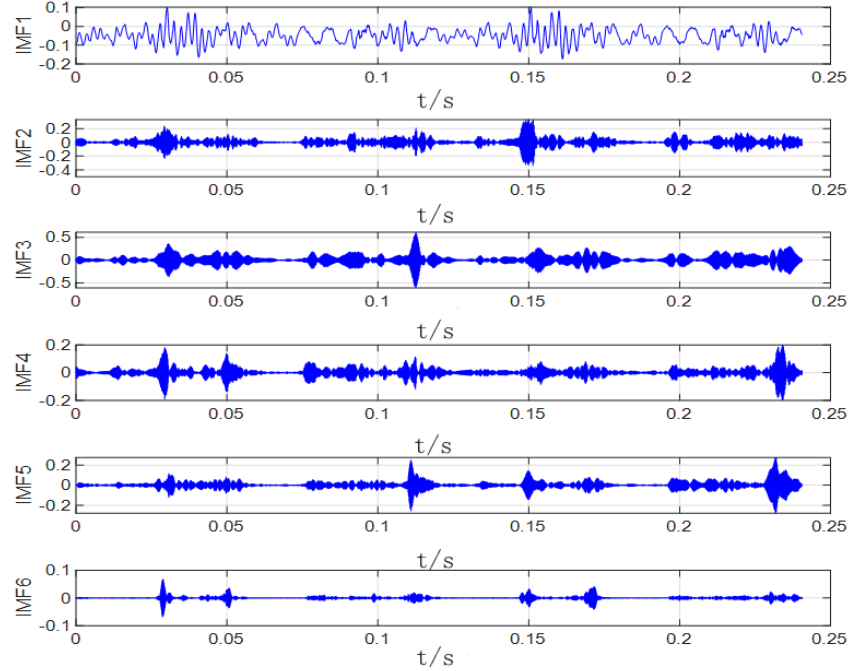


Fig 4 The decomposition results using original SSA-VMD

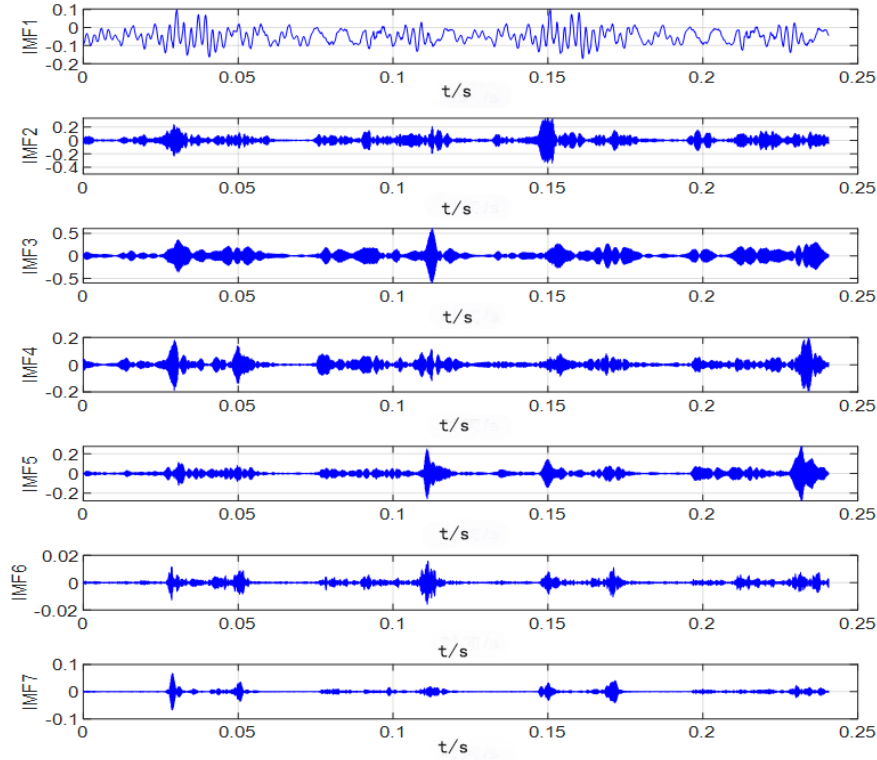


Fig 5 The decomposition results using improved SSA-VMD

From Figures 4 and 5, it can be observed that the SSA-VMD algorithm decomposes the vibration signal into six IMF components, whereas the improved SSA-VMD algorithm produces seven IMF components. This highlights a clear difference in the results of the two methods. However, Figures 4 and 5 alone do not provide enough evidence to conclusively determine which method performs better.

To further evaluate the two approaches, the IMF components obtained from both the SSA-VMD and improved SSA-VMD algorithms are continuing being processed. These IMF components with higher kurtosis values are selected for reconstruction. The fine composite multi-scale sample entropy (RCMSE) values of the reconstructed signals are then computed. The parameters for the RCMSE algorithm, as referenced in [14-15], are set with an embedding dimension  $m=2$  and a threshold  $r=0.20$ . The computed results are shown in Figures 6 and 7.

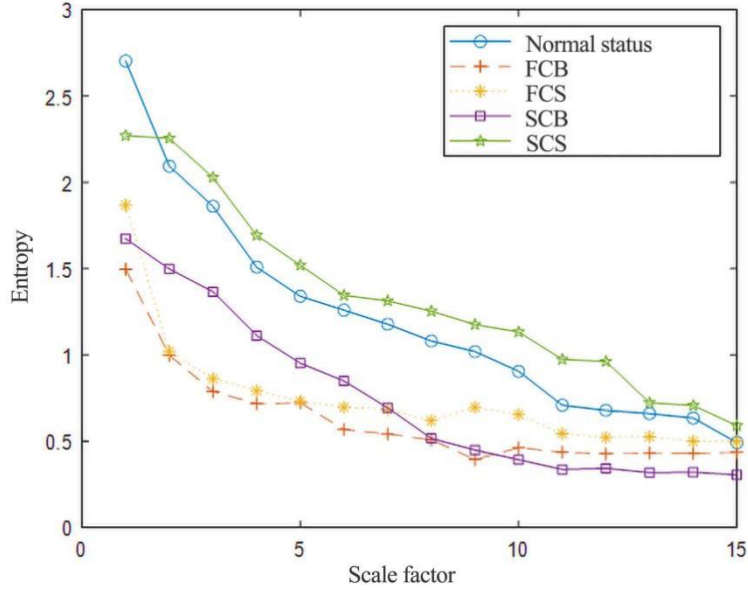


Fig 6 RCMSE curves of five working conditions calculated by SSA-VMD

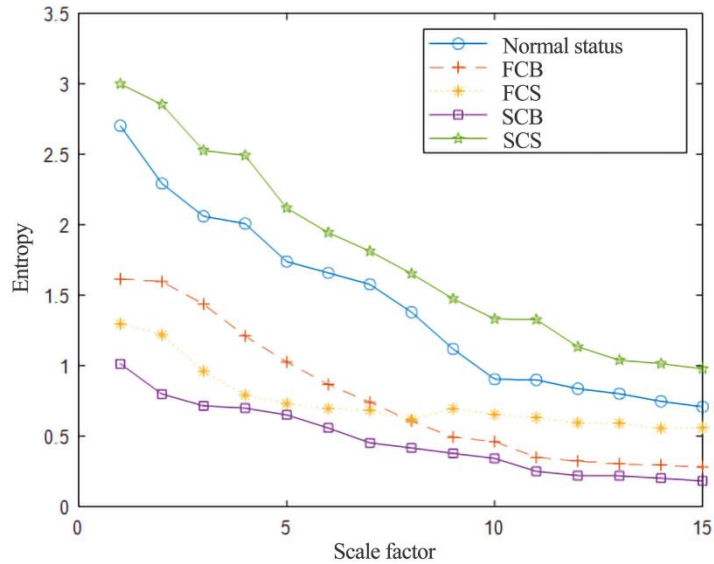


Fig 7 RCMSE curves of five working conditions calculated by improved SSA-VMD

As shown in Figures 6 and 7, the RCMSE entropy values for the five bearing conditions of the vehicle decrease as the scale factor  $\tau$  increases. The entropy distribution curves for the five bearing conditions obtained using the SSA-VMD method exhibit significant overlap across some intervals, which may affect the recognition of different fault states. In contrast, the entropy distribution curves for the five bearing conditions obtained using the improved SSA-VMD method show almost no overlap, allowing for a clearer and more intuitive distinction between the different fault states. Therefore, by reconstructing the signal and calculating the multi-scale

entropy curves, it is further demonstrated that the improved SSA-VMD method provides superior feature extraction compared to the original SSA-VMD method.

### 3.4 Fault Recognition Results

A total of 120 sample sets were collected from the vibration signals of the five different bearing conditions, with 70 random samples selected from each condition for the training set and the remaining 50 samples used for testing [16-18]. The initial parameter of the improved SSA-VMD algorithm was  $n=6$ ,  $\text{itermax}=10$ ,  $p=0.3$ . As can be seen in Table 2, the improved SSA-VMD method achieves a higher fault recognition accuracy. Experimental validation was performed using the vibration signals of the automotive bearings. The original SSA-VMD method and the improved SSA-VMD method were applied to decompose the vibration signals for the five different operating conditions of the bearings. Then, to denoise the original signal, the IMF components obtained from the decomposition were reconstructed, and the reconstructed signals were analyzed using RCMSE to extract feature vectors. Finally, a kernel extreme learning machine (KELM) was used to classify and recognize the extracted feature vectors, thereby diagnosing the fault types of the automotive bearings.

Table 2 The automotive bearings fault recognition accuracy

Type of data	SSA-VMD		Improved SSA-VMD	
	Accuracy rate (%)	Average accuracy (%)	Accuracy rate (%)	Average accuracy (%)
Normal	96.0		100.0	
FCB	98.0		98.0	
FCS	96.0	96.4	100.0	98.8
SCB	94.0		98.0	
SCS	98.0		98.0	

## 4. Conclusion

Automotive bearing fault diagnosis is a complex and critical task, as the safety of the vehicle directly impacts the driver's life. To improve the accuracy of automotive bearing fault diagnosis, this study proposes an enhanced SSA-VMD method, aimed at achieving higher fault recognition accuracy. A t-distribution mutation strategy is incorporated into the target position update process of the algorithm. The t-distribution operator strengthens the mutation ability, generating new mutated individuals to update the target position. This, in turn, improves the optimization capability of the SSA-VMD algorithm and enhances the precision of the optimization process. The proposed method was validated using vibration data from vehicle bearings. The results demonstrated that the average fault recognition accuracy of the improved SSA-VMD method is nearly 2% higher than that of the original SSA-VMD method, suggesting a significant improvement in diagnostic performance.

## Funding

Not applicable

**Author Contributions**

Conceptualization, Weidong Huang and Yiqun Cai; writing—original draft preparation, Weidong Huang and Yiqun Cai; writing—review and editing, Yiqun Cai; All of the authors read and agreed to the published the final manuscript.

**Institutional Reviewer Board Statement**

Not applicable

**Informed Consent Statement**

Not applicable

**Data Availability Statement**

Not applicable

**Conflict of Interest**

The authors declare no conflict of interest.

**Reference:**

- [1] L. Cao, J. Li, Z. Peng, et al. Fault diagnosis of rolling bearing based on EEMD and fast spectral kurtosis[J]. *Journal of Mechanical & Engineering*, 2021, 38: 1311-1316.
- [2] M. Li, C. Yan, W. Liu, et al. Fault diagnosis model of rolling bearing based on parameter adaptive AVMD algorithm[J]. *Applied Intelligence*, 2023, 53: 3150-3165.
- [3] K. Dragomiretskiy, D. Zosso. Variational mode decomposition[J]. *IEEE transactions on signal processing*, 2013, 62: 531-544.
- [4] H. Li, D. Li, H. Zhu, et al. An optimized VMD algorithm and its application in speech signal denoising[J]. *Journal of Jilin University*, 2021, 59: 1219-1227.
- [5] G. Huazhan, Z. Ying, S. Kai, et al., in Book *Fault Diagnosis of Rolling Bearing Based on SSA-VMD-WPT*, ed., ed. by Editor, IEEE, City, 2023, Chap. Chapter, pp. 1-6.
- [6] M. Qinghua, Z. Qiang. Improved sparrow algorithm combining Cauchy mutation and reverse learning[J]. *Computer Science Exploration*, 2021, 1-12.
- [7] L. Zhang, H. Li, D. Liu, et al. Identification and application of the most suitable entropy model for precipitation complexity measurement[J]. *Atmospheric Research*, 2019, 221: 88-97.
- [8] S. Lu, W. Gao, C. Hong, et al. A newly-designed fault diagnostic method for transformers via improved empirical wavelet transform and kernel extreme learning machine[J]. *Advanced Engineering Informatics*, 2021, 49: 101320.

[9] R. Jiao, S. Li, Z. Ding, et al. Fault diagnosis of rolling bearing based on BP neural network with fractional order gradient descent[J]. *Journal of Vibration Control*, 2024, 30: 2139-2153.

[10] J. Wang, Qin. Improved seagull optimization algorithm based on chaotic map and t-distributed mutation strategy[J]. *Appl. Res. Comput.*, 2022, 39: 170-176.

[11] X. Li, X. Peng, in Book A new non-destructive method for fault diagnosis of reciprocating compressor by measuring the piston rod strain, ed., ed. by Editor, IOP Publishing, City, 2019, Vol. 604, Chap. Chapter, pp. 012055.

[12] S. Xiao, A. Nie, Z. Zhang, et al. Fault diagnosis of a reciprocating compressor air valve based on deep learning[J]. *Applied Sciences*, 2020, 10: 6596.

[13] L. Zhang, L. Duan, X. Hong, et al., in Book Fault diagnosis method of reciprocating compressor based on domain adaptation under multi-working conditions, ed., ed. by Editor, IEEE, City, 2021, Chap. Chapter, pp. 588-593.

[14] L. ZHANG, L. DUAN, F. WAN. Residual network diagnosis method for reciprocating compressor fault[J]. *Journal of Electronic Measurement Instrumentation*, 2021, 35: 38-46.

[15] S. Gao, Q. Wang, Y. Zhang. Rolling bearing fault diagnosis based on CEEMDAN and refined composite multiscale fuzzy entropy[J]. *IEEE Transactions on Instrumentation Measurement*, 2021, 70: 1-8.

[16] B. Peng, Y. Bi, B. Xue, et al. A survey on fault diagnosis of rolling bearings[J]. *Algorithms*, 2022, 15: 347.

[17] H. Liu, F. Ke, Z. Zhang, et al. Fault Tolerance in Electric Vehicles Using Deep Learning for Intelligent Transportation Systems[J]. *Mobile Networks Applications*, 2023, 1-9.

[18] M. Guo, Y. Huang, Q. Zhao. Fault diagnosis method of rolling bearing based on IFD and KELM[J]. *Journal of Fuzhou University*, 2020, 48: 341-347.

© The Author(s) 2025. Published by Hong Kong Multidisciplinary Research Institute (HKMRI).



This is an Open Access article distributed under the terms of the Creative Commons Attribution License (<https://creativecommons.org/licenses/by/4.0>) which permits unrestricted use, distribution, and reproduction in any medium, provided the original work is properly cited.